Wind and Structures, *Vol. 20, No. 2 (2015) 169-189*
DOI: http://dx.doi.org/10.12989/was.2015.20.2.169

The impact of artificial discrete simulation of wind field on vehicle running performance

Mengxue Wu, Yongle Li* and Ning Chen

Department of Bridge Engineering, Southwest Jiaotong University, 610031 Chengdu, Sichuan, P.R. China

(Received November 18, 2014, Revised December 30, 2014, Accepted January 5, 2015)

Abstract. To investigate the effects of "sudden change" of wind fluctuations on vehicle running performance, which is caused by the artificial discrete simulation of wind field, a three-dimensional vehicle model is set up with multi-body dynamics theory and the vehicle dynamic responses in crosswind conditions are obtained in time domain. Based on Hilbert Huang Transform, the effects of simulation separations on time-frequency characteristics of wind field are discussed. In addition, the probability density distribution of "sudden change" of wind fluctuations is displayed, addressing the effects of simulation separation, mean wind speed and vehicle speed on the "sudden change" of wind fluctuations. The "sudden change" of vehicle dynamic responses, which is due to the discontinuity of wind fluctuations on moving vehicle, is also analyzed. With Principal Component Analysis, the comprehensive evaluation of vehicle running performance in crosswind conditions at different simulation separations of wind field is investigated. The results demonstrate that the artificial discrete simulation of wind field often causes "sudden change" in the wind fluctuations and the corresponding vehicle dynamic responses are noticeably affected. It provides a theoretical foundation for the choice of a suitable simulation separation of wind field in engineering application.

Keywords: artificial discrete simulation; sudden change; wind simulation separation; multibody dynamics; Hilbert Huang Transform; Principal Component Analysis

1. Introduction

In recent years, the high-speed rail transportation system in the world is experiencing a rapid development. The high speed and heavy transportation have a great influence on the safety of substructure (e.g., bridge) (Li *et al.* 2005, Yi *et al*. 2013). Moreover, the trend of high speed and light mass of vehicle make the safety and comfort of running vehicles in strong crosswind conditions of a great concern (Baker 2013, Cheli 2012, Diedrichs 2006, Wu *et al.* 2014). Some previous researches (Balzer 1977, Cooper 1984) have shown that the wind energy experienced by moving vehicles is different from that of the stationary vehicles when vehicles are operated at a high speed in strong crosswind conditions. In order to quantify vehicle dynamic responses in crosswind conditions so as to make proper assessment of the vehicle safety and comfort, the simulation of wind fluctuations for calculating the aerodynamic forces on moving vehicles is the key point.

*Corresponding author, Professor, E-mail: lele@swjtu.edu.cn

http://www.techno-press.org/?journal=was&subpage=8 ISSN: 1226-6116 (Print), 1598-6225 (Online)

Shinozuka and Deodatis (1991) presented the simulation of one-dimensional, uni-variate, stationary stochastic process by spectral representation method. Based on an extension of the spectral representation method, Deodatis (1996) proposed a simulation algorithm to generate sample functions of the stationary and multivariate stochastic processes corresponding to different locations in space according to its prescribed cross-spectral density matrix. For long-span bridges, it requires a large number of wind speed histories to be simulated and the total computational work is often too enormous to apply the spectral representation. Cao *et al*. (2000) and Li *et al*. (2004) introduce a practical method to simplify stochastic wind speed field for long-span bridges. Currently, in wind-vehicle-bridge coupling vibration system, the time histories of random wind speed fluctuations at finite discrete fixed-locations are generated with prescribed spectral characteristics (Cai and Chen 2004, Li *et al.* 2005, 2013, Xu and Ding 2006). The discrete fixed-location is referred as the simulation point and the distance between two adjacent points is referred as the simulation separation of wind field. This artificial discrete simulation of wind field will inevitably lead to discontinuity and "sudden change" in the wind fluctuations on running vehicles, which is clearly inconsistent with the actual situation. To ensure the continuity of simulated wind fluctuations for the calculation of aerodynamic forces on vehicles, the interpolation scheme may be used (e.g., Liu 2011). In addition, due to the high-speed vehicle motion, the actual wind fluctuation on moving vehicle is only a short-term wind velocity field. Therefore, the traditional wind field simulation based on fixed-point wind spectrum for calculating the aerodynamic forces on moving vehicles is computational too expensive. Based on Taylor's frozen turbulence hypothesis and isotropic turbulence model, the wind spectrum relative to moving vehicles is derived from the Kaimal spectrum of longitudinal wind fluctuation (Wu *et al.* 2014). Compared to the traditional wind field simulation based on fixed-point wind spectrum, the using of wind spectrum relative to moving vehicle can simulate the wind fluctuations more effectively for calculating the aerodynamic forces on moving vehicles. Meanwhile, the "sudden change" of wind fluctuations caused by artificial discrete simulation of wind field can be avoided. However, it should be noted that this framework cannot be easily applied in wind-vehicle-bridge system. Since the traditional approach is used in the simulation of wind fluctuations on bridge, it is difficult to combine the wind spectrum relative to moving vehicles with the traditional wind field simulation based on fixed-point wind spectrum into the wind-vehicle-bridge system. Therefore, the traditional wind field simulation based on fixed-point wind spectrum is still used most often to calculate the aerodynamic forces on moving vehicles in the current coupling vibration analysis of wind-vehicle-bridge system.

The "sudden change" of wind fluctuations occurs during the entire vehicle running process, which causes an additional vehicle dynamic response. As a result, the estimated vehicle dynamic responses are noticeably affected. It should be noted that the "sudden change" of wind fluctuations is sensitive to the simulation separation in the artificial discrete simulation of wind field. Different simulation separations may lead to significant differences in "sudden change" of wind fluctuations on running vehicles, thus affecting the vehicle dynamic responses in crosswind conditions. Theoretically, a small simulation separation results in a small "sudden change" of wind fluctuation. However, due to the limitation of computational efficiency, it is impossible to set the simulation separation too small. Therefore, comprehensively considering the computational efficiency and ensuring the accuracy for engineering application, it is of great importance to determine the appropriate simulation separation in the artificial discrete simulation of wind field.

In the present study, a three-dimensional vehicle model is set up with multibody dynamics theory. The wind fluctuation on moving vehicle is acquired from an efficient simulation algorithm of multivariate short-term stochastic wind velocity field and the vehicle dynamic responses in crosswind conditions are obtained in time domain. Based on Hilbert Huang Transform, the effects of simulation separations on time-frequency characteristics of wind field are discussed. In addition, the probability density distribution of “sudden change” of wind fluctuations is displayed, addressing the effects of simulation separation, mean wind speed and vehicle speed on the “sudden change” of wind fluctuations. The “sudden change” of vehicle dynamic responses, which is due to the discontinuity of wind fluctuations on moving vehicle, is also analyzed. With Principal Component Analysis, the comprehensive evaluation of vehicle running performance in crosswind conditions at different simulation separations of wind field is investigated.

2. Effects of simulation separation on characteristics of wind field

2.1 Wind fluctuations on moving vehicle using fixed -point wind spectrum

The time histories of random wind speed fluctuations at finite discrete fixed-locations are generated with the turbulence power spectral density (PSD) function and coherence function, e.g., the Kaimal spectrum (Eq. (1)) and the Davenport square-root coherence function (Eq. (2)). By applying an efficient simulation algorithm of multivariate short-term stochastic wind velocity field (Chen *et al.* 2014), the longitudinal component of fluctuating speed at discrete fixed-locations can be efficiently simulated. The PSD of *u*-component, $S_u(n)$, is given as the Kaimal spectrum (Kaimal *et al.* 1972), and the square-root coherence function, $Coh(n,\Delta r)$, is given as the Davenport formulation (Davenport 1961)

$$\frac{nS_u(n)}{u_*^2}=\frac{200\hat{n}}{(1+50\hat{n})^{5/3}} \tag{1}$$

where n is the frequency in Hz; $\hat{n}=nz/\overline{U}$ is the non-dimensional frequency; u_* is the shear velocity of the flow.

$$Coh(n,\Delta r)=\exp\left(-C\frac{n\Delta r}{\overline{U}}\right) \tag{2}$$

where Δr is a distance between adjacent simulation points; C is the decay constant related to wind correlation.

Fig. 1 shows an example of the obtained wind speed field of the longitudinal component as a function of time and space. The inclined line in Fig. 1 is an illustration to obtain the wind fluctuations of a point fixed on the moving vehicle. The time histories of random wind speed fluctuations at discrete fixed-locations are generated, which are represented by those colored lines in Fig. 1. When a vehicle is moving at a constant speed along the straight line of simulation points, a point fixed on the vehicle experiences a wind profile represented by the inclined line in Fig. 1, which is a function of the space-time distribution of both the longitudinal fluctuating component and the vehicle speed. When the point fixed on the vehicle arrives at a simulation point of wind field, the corresponding wind speed fluctuation at time t can be obtained from the time history of wind fluctuations at this simulation point. Once that the vehicle's position at each time step is known from the moving speed and trajectory, it is easy to obtain the time-history of the fluctuating wind speed of the moving point fixed on the vehicle, as shown in Fig. 2.

2.2 Effects of simulation separation on time-frequency characteristics of wind field

The random wind speed fluctuations at finite discrete fixed-locations are generated with prescribed spectral characteristics, which are stationary and Gaussian stochastic processes. However, due to the high-speed vehicle motion, the actual wind fluctuation on moving vehicle is only a short-term wind velocity field, which can appear to be non-stationary. The Hilbert Huang Transform (HHT) (Huang *et al.* 1998) offers a powerful and ideal method for non-stationary data analysis. Based on HHT method, the energy-frequency-time distribution, also referred as the Hilbert spectrum can be obtained. Fig. 3 displays the time histories of the fluctuating wind speed of *u*-component on moving vehicle at different simulation separations, where the mean wind speed is 20 m/s and the vehicle speed is 83.33 m/s. The corresponding Hilbert spectra of fluctuating wind speed on moving vehicle at the same mean wind speed and vehicle speed are shown in Fig. 4. As shown in Fig. 4, When the simulation separation is set as 1 m, 5 m, 10 m and 20 m, the main frequency range of wind energy is 0~0.5 Hz , 0~0.2 Hz, 0~0.1 Hz and 0~0.05 Hz, respectively.

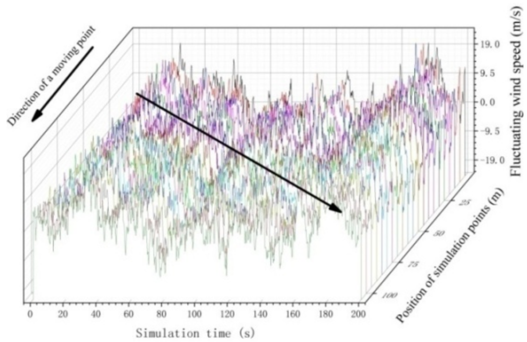

Fig. 1 The simulated longitudinal *u*-component as a function of time and space

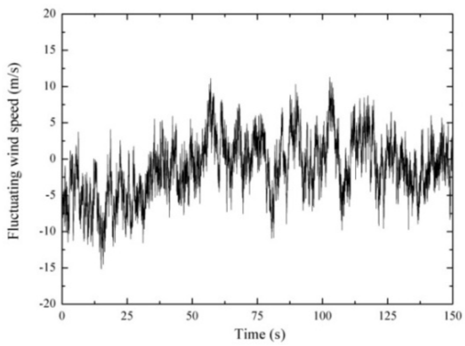

Fig. 2 The time-history of the fluctuating wind speed on moving vehicle

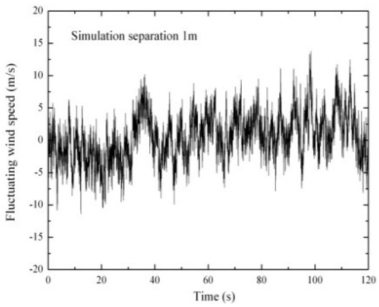

(a) Simulation separation: 1 m

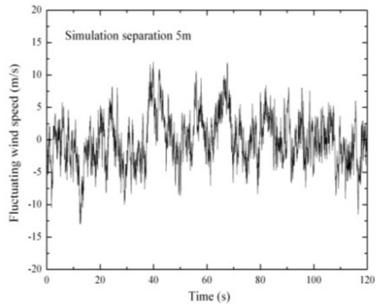

(b) Simulation separation: 5 m

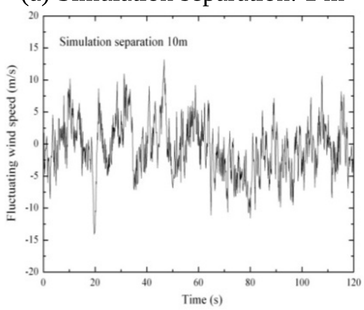

(c) Simulation separation: 10 m

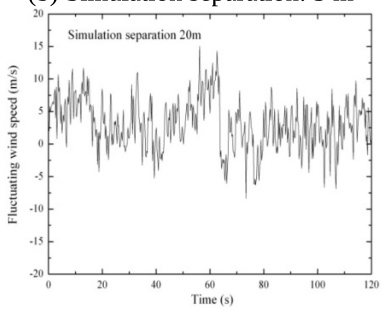

(d) Simulation separation: 20 m

Fig. 3 The time histories of *u*-component fluctuation on moving vehicle at different simulation separations

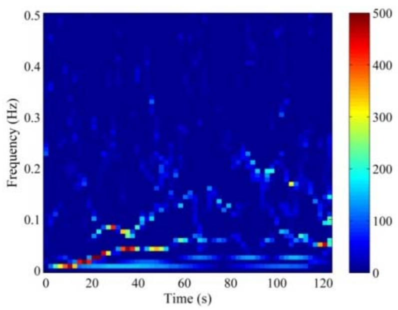

(a) Simulation separation: 1m

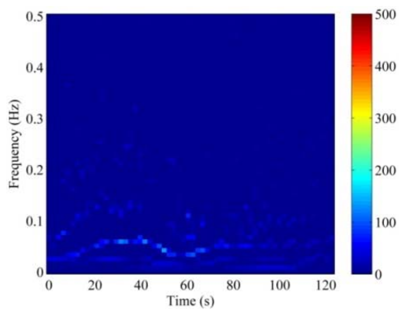

(b) Simulation separation: 5m

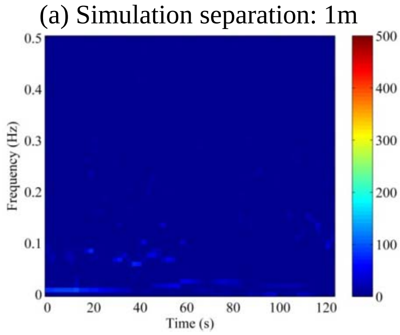

(c) Simulation separation: 10m

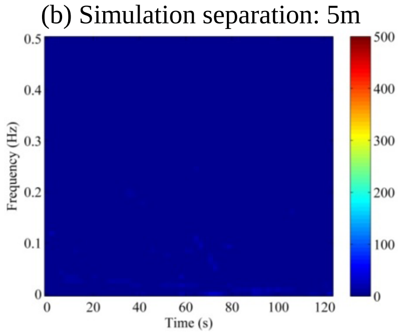

(d) Simulation separation: 20m

Fig. 4 The Hilbert spectrum of fluctuations on moving vehicle at different simulation separations

The results indicate that as the simulation separation increases, the frequency distribution range of wind energy decreases, and the high-frequency components of wind field are diminished or not included. In addition, the wind energy of fluctuations on moving vehicle significantly reduces with the increase of simulation separation.

2.3 Probability density distribution of “sudden change” of wind fluctuation on vehicle

The amplitude difference of the fluctuating wind speed on moving vehicle at adjacent time step can be used to estimate the “sudden change” of wind fluctuation on vehicle. In the present study, four different simulation separations (i.e., 1 m, 5 m, 10 m and 20 m) of wind field are considered. Fig. 5 shows the probability density distribution of the amplitude difference of the fluctuating wind speed on moving vehicle, where the mean wind speed is 10 m/s and 20 m/s, respectively, and the vehicle speed is 27.78 m/s. As shown in Fig. 5, the distribution range of probability density curve spreads more widely with the increase of simulation separation. When the simulation separation is small, the variation of the fluctuating wind speed on moving vehicle at adjacent time step is not significant, which makes it reasonable to assume that the wind fluctuations on running vehicle are continuous and therefore can represent the actual situation. Consequently, the effects of “sudden change” of wind fluctuations on vehicle caused by the artificial discrete simulation of wind field can be ignored. However, with the increase of simulation separation, the distribution range of probability density becomes wider and the variation of the fluctuating wind speed on moving vehicle at adjacent time step is more significant, indicating the necessity to consider the significant “sudden change” of wind fluctuation on vehicle. In general, the probability of the “sudden change” of wind fluctuations on running vehicle obviously increases with the increase of simulation separation. In addition, it also can be observed from Fig. 5 that the effects of “sudden change” of wind fluctuations on running vehicle caused by the artificial discrete simulation of wind field are even more significant as the mean wind speed increases. Fig. 6 displays the probability density distribution of the amplitude difference of the fluctuating wind speed on moving vehicle, where the mean wind speed is 20 m/s, and the vehicle speed is 27.78 m/s and 55.56 m/s, respectively. As shown in Fig. 6, the probability density distribution of the amplitude difference of the fluctuating wind speed on moving vehicle under the same mean wind speed 20 m/s is invariant with respect to the change of the vehicle speed. Therefore, the mean wind speed has a greater effect on “sudden change” of wind fluctuation on moving vehicle in comparison with vehicle speed.

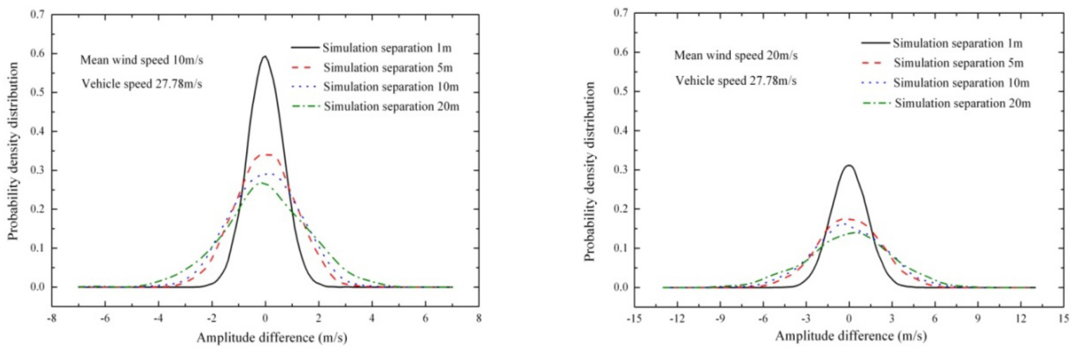

(a) Mean wind speed 10 m/s (b) Mean wind speed 20 m/s

Fig. 5 The effects of mean wind speed on “sudden change” of wind fluctuation on vehicle

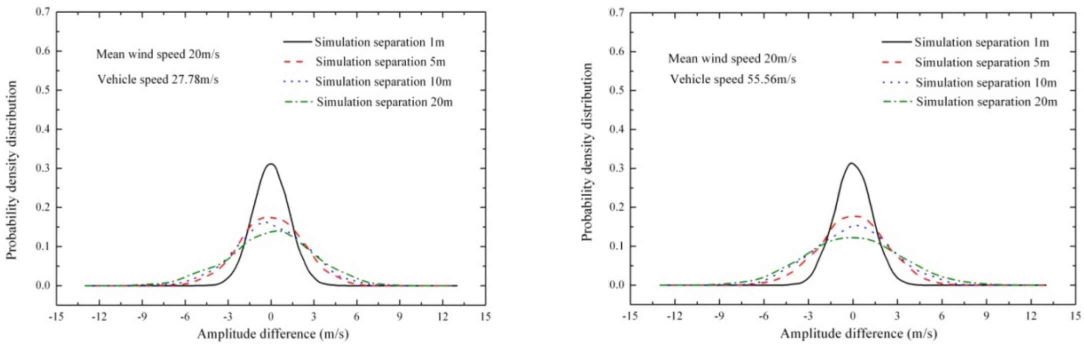

(a) Vehicle speed 27.78 m/s (b) Vehicle speed 55.56 m/s

Fig. 6 The effects of vehicle speed on “sudden change” of wind fluctuation on vehicle

3. Modeling and simulation of multibody dynamic model

3.1 The multibody model of the rail vehicle

In order to estimate the running performance of the rail vehicle, a 3D multibody system dynamics model of a high-speed passenger rail vehicle has been implemented in the Simpack Rail environment (a multibody analysis software widely used in the railway industry). The coach consists of one carbody, two bogie frames, and four wheelsets (two for each bogie). The multibody vehicle model is shown in Fig. 7. It takes into account all the significant degrees of freedom (DOF) of the system bodies. The inertial properties of the bodies are summarized in Table 1.

The vehicle model is equipped with two suspension stages, namely, the primary suspensions and the secondary suspensions. Both of these two suspension systems include appropriate elastic and damping elements to connect all the rigid bodies of the vehicle. For example, the primary suspension connects the wheelsets to the bogies, including springs and dampers, while the secondary suspension connects the carbody to the bogies, comprising the following elements: air springs, dampers, traction rod, anti-roll bar and lateral bump-stops. Both the primary suspensions and the secondary suspensions have been modeled by linear or nonlinear force elements to connect the rigid bodies. The main linear characteristics of the suspensions are shown in Table 2.

The natural frequency of the vehicle model is given in Table 3.

Table 1 Inertia properties of the multibody model

Body	Mass (kg)	Roll inertia ($kg\cdot m^2$)	Pitch inertia ($kg\cdot m^2$)	Yaw inertia ($kg\cdot m^2$)
Carbody	48,000	115,000	2,700,000	2,700,000
Bogie	3200	3200	7200	6800
Wheelset	2400	1200	200	1200

Table 2 Main linear stiffness and damping properties of the suspensions

Element	Longitudinal stiffness (N/m)	Lateral stiffness (N/m)	Vertical stiffness (N/m)	Longitudinal damping (Ns/m)	Lateral damping (Ns/m)	Vertical damping (Ns/m)
Primary suspension	9,000,000	3,000,000	1,040,000	--	--	30000
Secondary suspension	240,000	240,000	4,000,000	120,000	30,000	33330

Table 3 Modal properties of the vehicle model

Mode No.	Mode shape	Frequency (Hz)
1	Lower center roll & sway of carbody	0.5144
2	Vertical vibration of carbody	0.8288
3	Pitching vibration of carbody	0.9493
4	Yawing vibration of carbody	1.1953
5	upper center roll & sway of carbody	1.1963

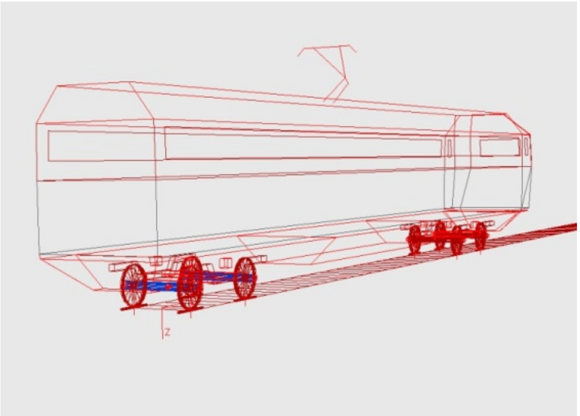

Fig. 7 Global view of the multibody model

3.2 Track irregularity of high-speed railway

The German track irregularity spectra for high-speed railway are chosen as inputs of excitation for the multibody system dynamics model. Track irregularities are usually classified into four types, namely vertical-profile, alignment, cross-level and gage irregularities. The gage irregularity is usually omitted in the vehicle analysis due to its weak effect. Considering the focus of this study is mainly on the effects of “sudden change” of wind fluctuations on vehicle dynamic responses, the vertical-profile (Eq. (3)) and alignment irregularities (Eq. (4)) are then used as inputs of excitation for kinetic simulation of high-speed vehicle.

The comparison of simulated power spectral density (PSD) and the corresponding target spectrum is shown in Fig. 8. It is shown that the simulated PSD is consistent with its target.

Vertical-profile irregularity:
$$S_v(\Omega)=\frac{A_v\Omega_c^2}{\left(\Omega^2+\Omega_r^2\right)\left(\Omega^2+\Omega_c^2\right)} \tag{3}$$

Alignment irregularity:
$$S_a(\Omega)=\frac{A_a\Omega_c^2}{\left(\Omega^2+\Omega_r^2\right)\left(\Omega^2+\Omega_c^2\right)} \tag{4}$$

where Ω is the space frequency; A_a (= 2.119×10^{-7} m·rad) and A_v (= 4.032×10^{-7} m·rad) are the roughness parameters; Ω_c (= 0.8246 rad/m) and Ω_r (=0.0206 rad/m) are the break frequencies.

3.3 Aerodynamic forces on moving vehicles

It is assumed that the mean wind velocity is normal to the direction of the vehicle movement. Neglecting self-excited loads on the vehicle, the static wind loads and buffeting loads are taken into account. Only three components of aerodynamic forces on the vehicle, namely, side force *D*, lift force *L* and rolling moment *M* are considered in the analysis of vehicle dynamic responses in crosswind conditions, as shown in Fig. 9.

The aerodynamic coefficients can be directly measured by the moving vehicle model in a wind tunnel, however, such a test with a moving vehicle model is very difficult (Cooper 1981, Baker 1986, Li *et al.* 2014). For a ground vehicle, the aerodynamic coefficients can be measured by wind tunnel tests with a certain yaw angle representing the effect of vehicle movement (Cooper 1981, Suzuki *et al*. 2003). In this study, the aerodynamic coefficients of the vehicle are calculated as Eqs. (5)-(7) and the measured static aerodynamic coefficients of the vehicle model are listed in Table 4.

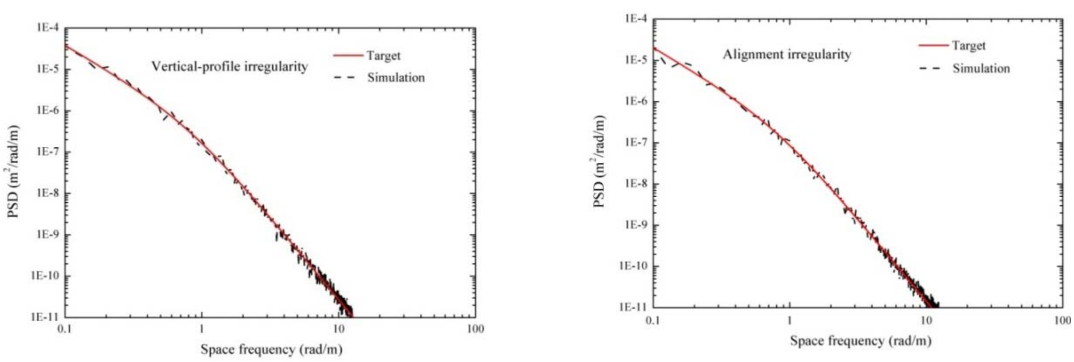

(a) Vertical-profile irregularity (b) Alignment irregularity

Fig. 8 The PSD of Vertical-profile and alignment irregularities

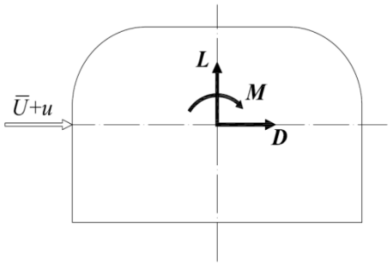

Fig. 9 Convention of wind velocity and aerodynamic forces

$$C_D(\alpha)=\frac{F_D}{1/2\rho\bar{U}^2 HL} \tag{5}$$

$$C_L(\alpha)=\frac{F_L}{1/2\rho\bar{U}^2 BL} \tag{6}$$

$$C_M(\alpha)=\frac{F_M}{1/2\rho\bar{U}^2 B^2 L} \tag{7}$$

where $C_D(\alpha)$, $C_L(\alpha)$ and $C_M(\alpha)$ are the side force coefficient, lift force coefficient and rolling moment coefficient, respectively; α is the efficient angle of incidence (in the present study, the vertical fluctuation is neglected, then $\alpha = 0^\circ$); F_D, F_L and F_M are the side force, lift force and rolling moment measured by the force balance; H is the cross-wind projected area (per unit length) of vehicle model normal to the main stream direction; B is the width of vehicle model along the mean wind direction; L is the length of vehicle model.

Referring to the literature (Li *et al.* 2005), the cosine rule can be approximately used to determine the wind loads on vehicle, and the aerodynamic forces per unit length on the vehicle are given as Eqs. (8)-(10)

Side force *D*: $$D=\frac{1}{2}\rho HC_D(\alpha)\bar{U}^2+\rho HC_D(\alpha)\bar{U}u \tag{8}$$

Lift force *L*: $$L=\frac{1}{2}\rho BC_L(\alpha)\bar{U}^2+\rho BC_L(\alpha)\bar{U}u \tag{9}$$

Rolling moment *M*: $$M=\frac{1}{2}\rho B^2 C_M(\alpha)\bar{U}^2+\rho B^2 C_M(\alpha)\bar{U}u \tag{10}$$

where ρ is the air density; $\bar{U}$ is the mean wind speed; u is the longitudinal fluctuation velocity acting on moving vehicle.

Table 4 Aerodynamic coefficients of vehicle model

Aerodynamic coefficients	C_D	C_L	C_M
Vehicle	0.6006	1.2446	0.0348

In the present study, the aerodynamic forces are treated as the inputs of excitation which are varied with time for kinetic simulation of high-speed vehicle under cross wind in the Simpack Rail environment.

4. Effects of "sudden change" of wind fluctuations on vehicle dynamic responses

4.1 The case without track irregularities

In order to demonstrate the influences of “sudden change” of wind fluctuations caused by artificial discrete simulation of wind field on vehicle dynamic performance, the lateral and vertical accelerations of the vehicle body, the reduction rate of vertical wheel loads on left wheel and the derailment coefficient at different simulation separations of wind field are compared in Fig. 10, where the mean wind speed is 20 m/s and the vehicle speed is 83.33 m/s. It should be noted that the “sudden change” of wind fluctuations is very sensitive to the simulation separation in the artificial discrete simulation of wind field. Different simulation separations may lead to significant differences in the “sudden change” of wind fluctuations on running vehicles. As shown in Fig. 10, it can be observed that simulation separation has a significant influence on the vehicle dynamic responses in crosswind conditions.

The amplitude difference of the dynamic responses of vehicle at adjacent simulation point of wind field can be used to estimate the effects of the “sudden change” of wind fluctuation on vehicle running performance. Fig. 11 displays the probability density distribution of the amplitude difference of the dynamic responses of vehicle, where the mean wind speed is 20 m/s and the vehicle speed is 83.33 m/s. When the simulation separation is small, the variation of the dynamic responses of vehicle at adjacent simulation point of wind field is not significant, which indicates that the effects of “sudden change” of wind fluctuations on vehicle caused by the artificial discrete simulation of wind field are relatively weak, and the additional dynamic effects appended to vehicle is not obvious. However, with the increase of simulation separation, the distribution range of probability density curve spreads more widely and the variation of the dynamic responses of vehicle at adjacent simulation point is more significant, indicating that the “sudden change” of wind fluctuation on vehicle cannot be ignored. Therefore, the simulation separation of wind field has a significant influence on the vehicle dynamic responses in crosswind conditions, especially on the lateral acceleration, reduction rate of vertical wheel loads and derailment coefficient.

4.2 The case with track irregularities

Both the track irregularities and the aerodynamic forces are treated as inputs of excitation and a kinetic simulation of high-speed vehicle in crosswind conditions at the speed of 55.56 m/s is performed. Figs. 12(a), 13(a), 14(a) and 15(a) display the time histories of dynamic responses of vehicle at different simulation separations of wind field, where the mean wind speed is 10 m/s.

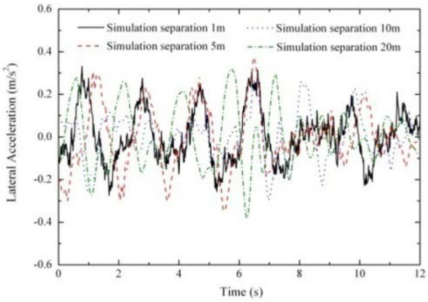

(a) Lateral Acceleration

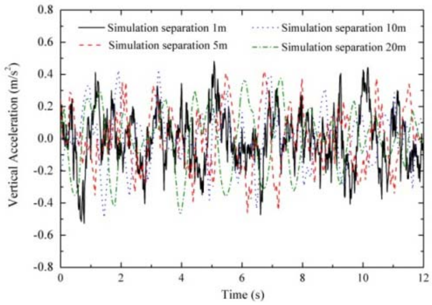

(b) Vertical Acceleration

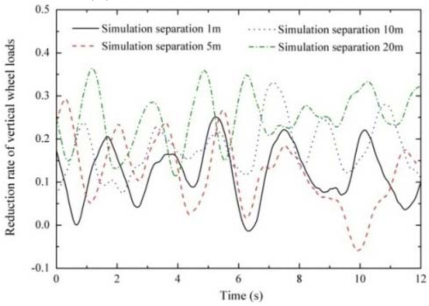

(c) Reduction rate of vertical wheel loads

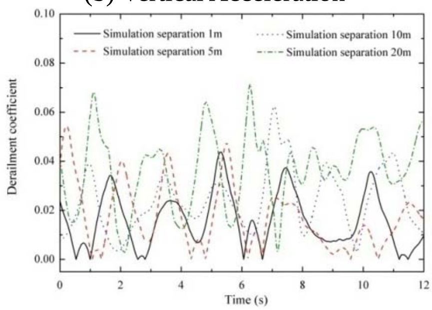

(d) Derailment coefficient

Fig. 10 Time histories of vehicle dynamic responses at different simulation separations

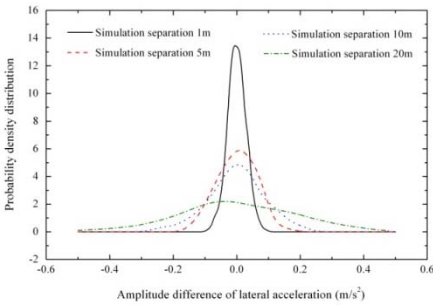

(a) Lateral Acceleration

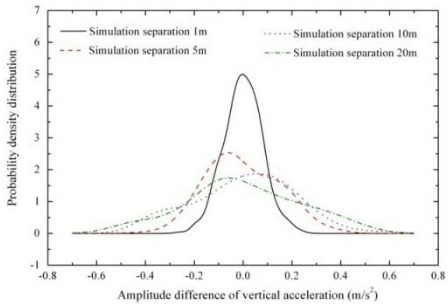

(b) Vertical Acceleration

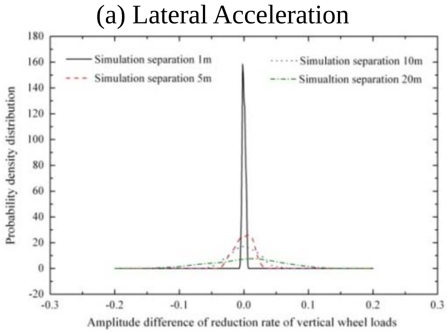

(c) Reduction rate of vertical wheel loads

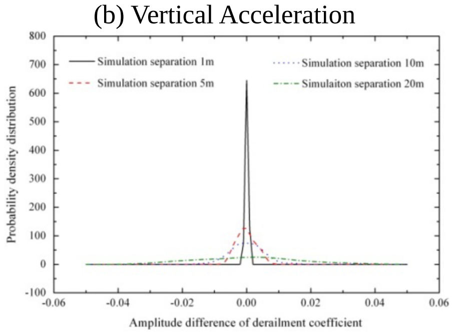

(d) Derailment coefficient

Fig. 11 The probability density distribution of the amplitude difference of the dynamic responses of vehicle

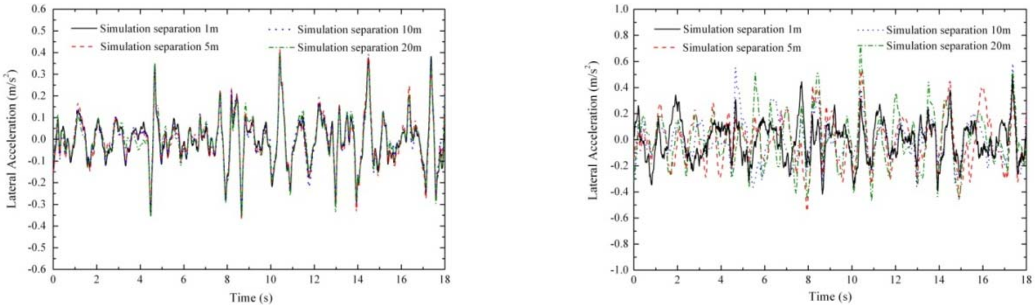

(a) Mean wind speed 10 m/s (b) Mean wind speed 20 m/s

Fig. 12 Time histories of lateral acceleration at different mean wind speeds

It can be seen from these figures that the influences of simulation separation on the dynamic responses of vehicle are not obvious. Figs. 12(b), 13(b), 14(b) and 15(b) display the time histories of dynamic responses of vehicle at different simulation separations of wind field, where the mean wind speed is 20 m/s. However, in the case where the mean wind speed is 20 m/s, it can be observed that the simulation separation has a significant influence on the vehicle dynamic responses in crosswind conditions. With both the track irregularities and the aerodynamic forces existing, when the mean wind speed is small, the track irregularities may have a predominant effect on dynamic responses of vehicle, while the influence of simulation separation is not significant.

Fig. 16 displays the probability density distribution of the amplitude difference of the dynamic responses of vehicle at vehicle speed of 55.56 m/s, where the mean wind speed is 20 m/s. As shown in Fig. 16, it can be observed that the influence of simulation separation of wind field on the reduction rate of vertical wheel loads is not significant, which is different from the case without track irregularities. Fig. 17 shows the effects of track irregularities on the probability density distribution of the amplitude difference of lateral acceleration of vehicle, where the vehicle speed is 55.56 m/s and the mean wind speed is 10 m/s. As shown in Fig. 17(b), the probability density distribution curves of the amplitude difference of lateral acceleration of vehicle are very similar at simulation separations of 5 m, 10 m and 20 m, which is very different from those in Fig. 17(a). The existence of track irregularities may make the question about the impacts of “sudden change” of wind fluctuations on vehicle dynamic responses more complicated.

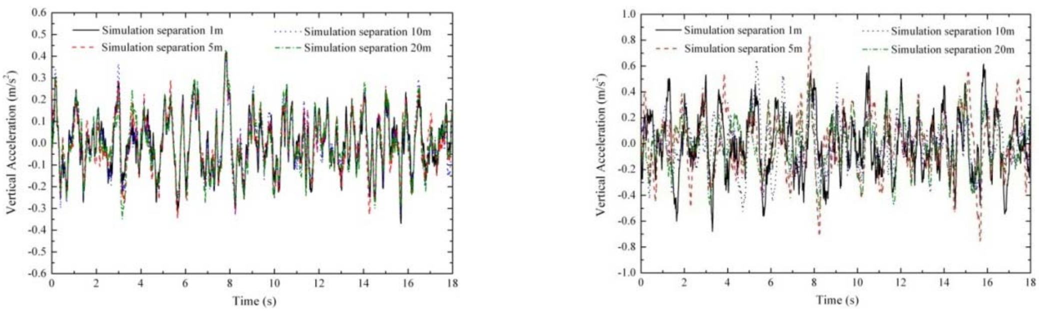

(a) Mean wind speed 10m/s (b) Mean wind speed 20m/s

Fig. 13 Time histories of vertical acceleration at different mean wind speeds

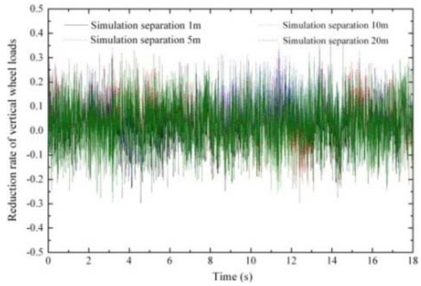

(a) Mean wind speed 10 m/s

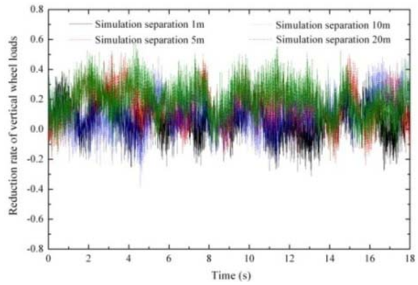

(b) Mean wind speed 20 m/s

Fig. 14 Time histories of reduction rate of vertical wheel loads at different mean wind speeds

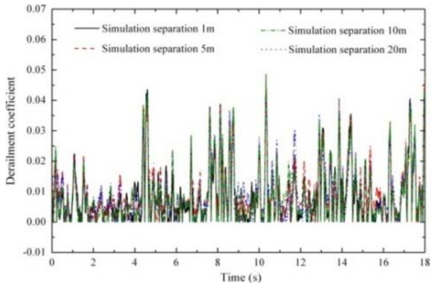

(a) Mean wind speed 10 m/s

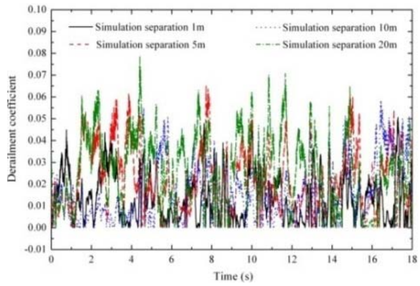

(b) Mean wind speed 20 m/s

Fig. 15 Time histories of derailment coefficient at different mean wind speeds

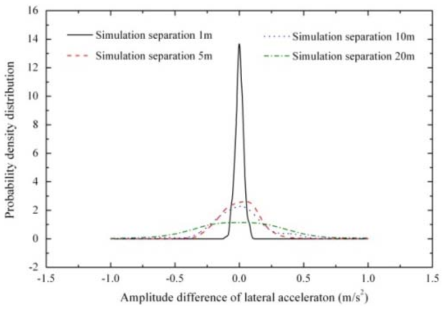

(a) Lateral acceleration

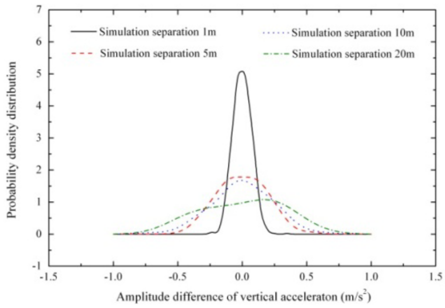

(b) Vertical acceleration

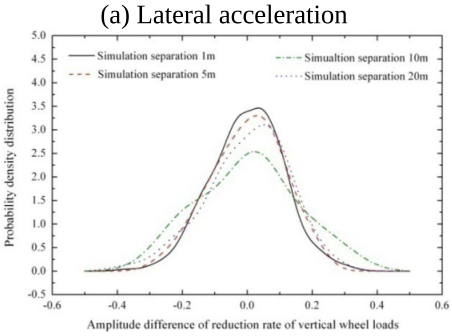

(c) Reduction rate of vertical wheel loads

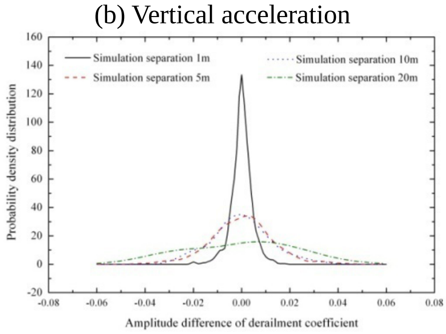

(d) Derailment coefficient

Fig. 16 The probability density distribution of the amplitude difference of the vehicle dynamic responses

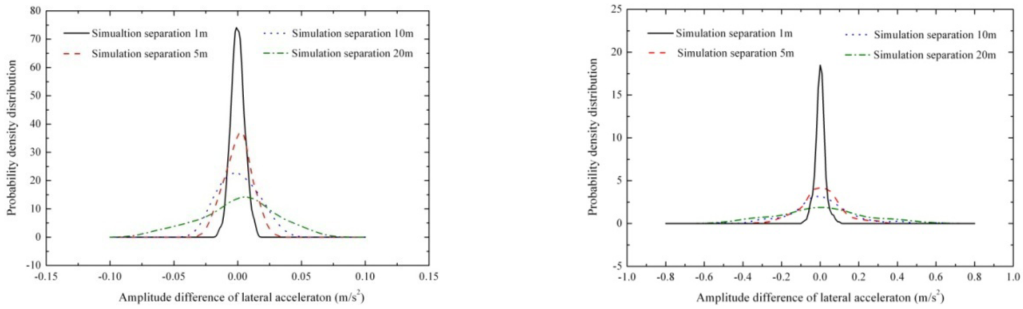

(a) Without track irregularities (b) With track irregularities

Fig. 17 The effects of track irregularities on the probability density distribution of the amplitude difference of the vehicle dynamic responses

5. Comprehensive evaluation of vehicle running performance at different simulation separations

The above discussions have shown that the “sudden change” of wind fluctuations may cause an additional vehicle dynamic response, which may not well represent the actual performance of vehicles in crosswind conditions. Noting that the “sudden change” of wind fluctuations is very sensitive to the simulation separation in the artificial discrete simulation of wind field, it is reasonable to evaluate the vehicle running performance with respect to different simulation separations. In the present study, the comprehensive evaluation of vehicle running performance at different simulation separations is performed, in order to provide a theoretical foundation for the choice of a suitable simulation separation of wind field in engineering application.

In the present study, the lateral acceleration, vertical acceleration, reduction rate of vertical wheel loads and derailment coefficient are chosen as the indexes to represent the dynamic responses of the vehicle. In order to estimate the influences of “sudden change” of wind fluctuations on vehicle running performance, eight indexes (all the values are absolute values) are used as the inputs, as shown in Table 5. The eight indexes can be treated as sets of vector, which varies with respect to different simulation separations of wind field. A comprehensive evaluation is performed, in order to investigate the running performance of vehicle in crosswind conditions at different simulation separations of wind field. The Principal Component Analysis is adopted to realize the comprehensive evaluation.

5.1 Principal component analysis

The principal component analysis (PCA) is a simple and widely used technique to reduce the dimensionality of a data set consisting of a large number of interrelated variables, while retaining as much as possible of the variance contained in the data set. This is achieved by transforming the original set of correlated variables to a new set of variables, namely the principal components, which are uncorrelated. Ordering the eigenvalues of the transformation decreasingly, the first few principal components retain most of the variance present in all of the original variances (Jolliffe 2002).

Table 5 Indexes to estimate the influences of "sudden change" of wind fluctuations on vehicle running performance

Lateral Acceleration (m/s^2)	Maximum
	Maximum of amplitude difference at adjacent simulation point
Vertical Acceleration (m/s^2)	Maximum
	Maximum of amplitude difference at adjacent simulation point
Reduction rate of vertical wheel loads	Maximum
	Maximum of amplitude difference at adjacent simulation point
Derailment coefficient	Maximum
	Maximum of amplitude difference at adjacent simulation point

In the present study, for 4 kinds of simulation separations of wind field, namely, 1m, 5m, 10m and 20 m, the values of eight indexes are obtained from the vehicle multibody dynamic simulation. This resulted in a 4×8 data matrix. Since the eight indexes have different dimensions and order of magnitude, it is necessary to standardize the original index data to eliminate the impacts of dimension and order of magnitude, and ensure the reliability of the results. The standardized equation is given as Eq. (11).

$$x_{ij}^* = \frac{x_{ij} - \bar{x}_j}{\sqrt{\mathrm{var}(x_j)}} \qquad (i = 1, 2, \dots, n; j = 1, 2, \dots, p) \tag{11}$$

where x_{ij}^* is the standardized index data; x_{ij} is the original index data; n represents the number of samples, which is $n = 4$ in the present study; p represents the number of indexes, which is $p = 8$ in the present study; $\bar{x}_j = \frac{1}{n}\sum_{i=1}^{n} x_{ij}$; $\mathrm{var}(x_j) = \frac{1}{n-1}\sum_{i=1}^{n}(x_{ij} - \bar{x}_j)^2$.

All pairs of the 8 column standardized vectors of this matrix are inter-correlated using Pearson's coefficient of correlation. The resulting correlation matrix (8×8), with unity in the diagonal, is subjected to the principal component analysis (Eigenvalue Decomposition). The eigenvalues of the correlation matrix are just the variations of the corresponding principal components. With the eigenvalues (i.e., the variance of principal component) decreasingly, the relevant information retained by principal components also decreases. Therefore, only the first few principal components retaining most of the variation are chosen to extract the relevant information from the original confusing data sets. The component scores are then calculated using Eq. (12)

$$F = Z \times V \tag{12}$$

where F is the matrix of component scores; Z is the matrix of standardized index data; V is the matrix of eigenvectors.

Finally, the comprehensive evaluation score of each sample is calculated based on the selected principal components, using Eq. (13). The comprehensive evaluation score can reflect the influences of “sudden change” of wind fluctuations caused by artificial discrete simulation of wind field on vehicle running performance.

$$F_{CE} = \sum_{g=1}^{k} \lambda_g F_g \tag{13}$$

where F_{CE} is the comprehensive evaluation score; F_g is the principal component score; k represents the number of selected principal components; λ_g represents the percentage of the variance of the g^{th} principal component in the total variance.

5.2 Example

Without track irregularities, a kinetic simulation of high-speed vehicle in crosswind conditions at the speed of 27.78 m/s is performed, where the mean wind speed is 10 m/s. Table 6 shows the eight sets of original index data at different simulation separations of wind field, which are obtained from the dynamic responses of vehicle. Table 6 resulted in a 4×8 original data matrix. After standardizing the original index data, the standardized data will be applied in the following principal component analysis, using the procedure described in the Section 5.1.

The comprehensive evaluation scores at different simulation separations of wind field are shown in Table 7, where F_{CE} represents the comprehensive evaluation score. The comprehensive evaluation score can reflect the influences of “sudden change” of wind fluctuations caused by artificial discrete simulation of wind field on vehicle running performance. The higher comprehensive evaluation score indicates the stronger impacts of “sudden change” of wind fluctuations on vehicle running performance. This table shows that the comprehensive evaluation score increases with the increasing simulation separation, indicating the stronger impacts of “sudden change” of wind fluctuations on vehicle running performance.

5.3 Results and analysis

As mentioned in the Section 4.2, the track irregularities may make the impacts of “sudden change” of wind fluctuations on the dynamic responses of running vehicle more complicated. In the present study, the comprehensive evaluation of vehicle running performance at different simulation separations of wind field is only performed without considering the track irregularities.

Fig. 18 shows the comprehensive evaluation scores at different simulation separations of wind field, where the vehicle speed is 27.78 m/s and 55.56 m/s, and the mean wind speed is 10 m/s and 20 m/s, respectively. It can be seen that the comprehensive evaluation score increases with the increase of simulation separation, indicating the stronger impacts of “sudden change” of wind fluctuations on vehicle running performance. In addition, the slope of the variation of comprehensive evaluation score between each two adjacent simulation separations can reflect the level of impact of simulation separation on vehicle running performance in crosswind conditions. The higher slope indicates that the variation of simulation separation results in the more significant variation of vehicle running performance.

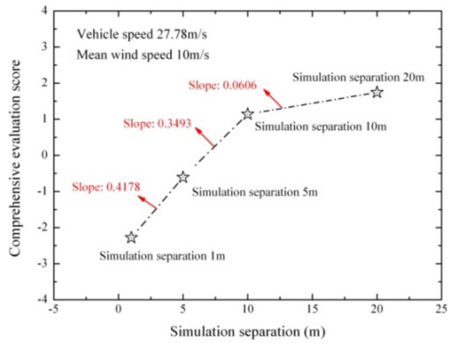

(a) Vehicle speed 27.78 m/s, Mean wind speed 10 m/s

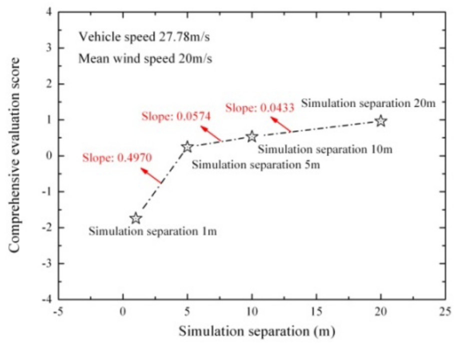

(b) Vehicle speed 27.78 m/s, Mean wind speed 20 m/s

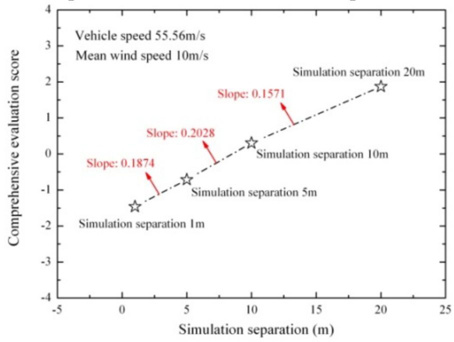

(c) Vehicle speed 55.56 m/s, Mean wind speed 10 m/s

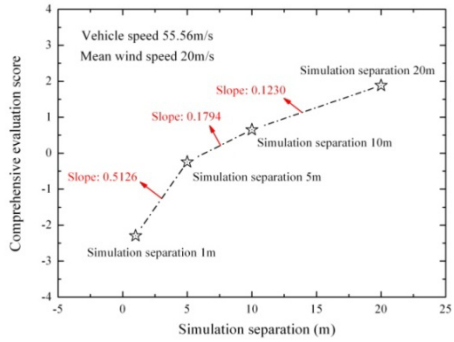

(d) Vehicle speed 55.56 m/s, Mean wind speed 20 m/s

Fig. 18 The comprehensive scores at different vehicle speeds and mean wind speeds

Table 6 Eight sets of original index data at different simulation separations

Eight Indexes		Simulation separation			
		1 m	5 m	10 m	20 m
Lateral Acceleration (m/s^2)	Max	0.0550	0.0522	0.0508	0.0364
	Max of amplitude difference	0.0182	0.0481	0.0619	0.0694
Vertical Acceleration (m/s^2)	Max	0.1084	0.0897	0.0697	0.0444
	Max of amplitude difference	0.0564	0.0787	0.0910	0.0778
Reduction rate of vertical wheel loads	Max	0.0787	0.0831	0.0758	0.0715
	Max of amplitude difference	0.0030	0.0147	0.0283	0.0324
Derailment coefficient	Max	0.0079	0.0092	0.0082	0.0067
	Max of amplitude difference	0.0005	0.0027	0.0052	0.0045

Table 7 The comprehensive evaluation scores at different simulation separations

Sample	F_{CE}
Simulation separation 1 m	-2.2781
Simulation separation 5 m	-0.6069
Simulation separation 10 m	1.1397
Simulation separation 20 m	1.7452

6. Conclusions

- This study investigates the impacts of artificial discrete simulation of wind field on vehicle running performance. Based on Hilbert Huang Transform, the effects of different simulation separations of wind field on the time-frequency characteristics of wind field are discussed. The frequency distribution range of wind energy decreases with the increase of simulation separation, and the high-frequency components of wind field are diminished or not included. In addition, the wind energy of fluctuations on moving vehicle significantly reduces with the increase of simulation separation.
- The amplitude difference of the fluctuating wind speed on moving vehicle at adjacent time step can be used to estimate the "sudden change" of wind fluctuation on vehicle. The distribution range of probability density curve spreads more widely with the increase of simulation separation. In general, the probability of the "sudden change" of wind fluctuation on running vehicle obviously increases with the increase of simulation separation. It should be noted that mean wind speed has a greater effect on "sudden change" of wind fluctuation on moving vehicle in comparison with vehicle speed.
- In the case without track irregularities, the simulation separation of wind field has a significant influence on the vehicle dynamic responses in crosswind conditions. However, with both the track irregularities and the aerodynamic forces existing, when the mean wind speed is small, the track irregularities may have a predominant effect on dynamic responses of vehicle, while the influence of simulation separation is not significant. The existence of track irregularities may make the question about the impacts of "sudden change" of wind fluctuations on vehicle dynamic responses more complicated.
- With Principal Component Analysis, the vehicle running performance in crosswind conditions at different simulation separations of wind field can be comprehensively evaluated. The comprehensive evaluation score increases with the increase of simulation separation, indicating the stronger impacts of "sudden change" of wind fluctuations on vehicle running performance. It can provide a theoretical foundation for the choice of a suitable simulation separation of wind field in engineering application.

Acknowledgements

The authors are grateful for the financial supports from the National Natural Science

Foundation of China under Grant NNSF-U1334201, 51278434, the Sichuan Province Youth Science and Technology Innovation Team (2015TD0004), the National Key Basic Research Development Plan of China (2013CB036206) and the National Key Technology R&D Program (2012BAG05B02).

References

Baker, C.J. (1986), "Train aerodynamic forces and moments from moving model experiments", *J. Wind Eng. Ind. Aerod.*, **24**(3), 227-251.

Baker, C.J. (2013), "A framework for the consideration of the effects of crosswinds on trains", *J. Wind Eng. Ind. Aerod.*, **123**, 130-142.

Balzer, L.A. (1977), "Atmospheric turbulence encountered by high-speed ground transport vehicles", *J. Mech. Eng. Sci.*, **19**, 227-235.

Cai, C.S. and Chen, S.R. (2004), "Framework of vehicle–bridge–wind dynamic analysis", *J. Wind Eng. Ind. Aerod.*, **92**(7-8), 579-607.

Cao, Y.H., Xiang, H.F. and Zhou, Y. (2000), "Simulation of stochastic wind velocity field on long-span bridges", *J. Eng. Mech. - ASCE*, **126**(1), 1-6.

Cheli, F., Corradi, R. and Tomasini, G. (2012), "Crosswind action on rail vehicles: A methodology for the estimation of the characteristic wind curves", *J. Wind Eng. Ind. Aerod.*, **104-106**, 248-255.

Chen, N., Li, Y.L. and Xiang, H.Y. (2014), "A new simulation algorithm of multivariate short-term stochastic wind velocity field based on inverse fast Fourier transform", *Eng. Struct.*, **80**, 251-259.

Cooper, R.K. (1981), "The effect of cross-winds on trains", *J. Fluid. Eng. - T ASME*, **103**(1), 170-178.

Cooper, R.K. (1984), "Atmospheric turbulence with respect to moving ground vehicles", *J. Wind Eng. Ind. Aerod.*, **17**(2), 215-238.

Davenport, A.G. (1962), "The spectrum of horizontal gustiness near the ground in high winds", *Q. J. Roy. Meteorol. Soc.*, **88**(376), 197-198.

Deodatis, G. (1996), "Simulation of ergodic multivariate stochastic processes", *J. Eng. Mech. - ASCE*, **122**(8), 778-787.

Diedrichs, B. (2006), *Studies of two aerodynamics effects on high-speed trains crosswind stability and discomforting car body vibrations inside tunnels*, Ph.D. Dissertation, Aeronautical and Vehicle Engineering, Royal Institute of Technology, Stockholm, Sweden.

Huang, N.E., Shen, Z., Long, S.R., Wu, M.C., Shih, H.H., Zheng, Q., Yen, N.C., Tung, C.C. and Liu, H.H. (1998), "The empirical mode decomposition and the Hilbert spectrum for nonlinear and non-stationary time series analysis", *P. R. Soc. Lond.*, **454**, 903-995.

Jolliffe, I.T. (2002), *Principal component analysis*, Springer, New York.

Kaimal, J.C., Wyngaard, J.C., Izumi, Y. and Cote, O.R. (1972), "Spectral characteristics of surface-layer turbulence", *Q. J. Roy. Meteorol. Soc.*, **98**(417), 563-589.

Li, Y.L., Liao, H.L. and Qiang, S.Z. (2004), "Simplifying the simulation of stochastic wind velocity fields for long cable-stayed bridges", *Comput. Struct.*, **80**(20-21), 1591-1598.

Li, Y.L., Qiang, S.Z., Liao, H.L. and Xu, Y.L. (2005), "Dynamics of wind-rail vehicle-bridge systems", *J. Wind Eng. Ind. Aerod.*, **93**(6), 483-507.

Li, Y.L., Xiang, H.Y., Wang, B., Xu, Y.L. and Qiang, S.Z. (2013), "Dynamic analysis f wind-vehicle-bridge system with two trains interaction", *Adv. Struct. Eng.*, **16**(10), 1663-1670.

Li, Y.L., Hu, P., Xu, Y.L., Zhang, M.J. and Liao, H.L. (2014), "Wind loads on a moving vehicle–bridge deck system by wind-tunnel model test", *Wind. Struct.*, **19**(2), 145-167.

Liu, H.T. (2011), *Dynamic responses of coupled train, automobile and bridge system under strong wind and analysis of running safety and riding comfort of vehicles*, Ph.D. Dissertation, Bridge and Tunnel Engineering, Central South University, Hunan. (in Chinese)

Shinozuka, M. and Deodatis, G. (1991), "Simulation of stochastic processes by spectral representation",

Appl. Mech. Rev., **44**(4), 191-204.
Suzuki, M., Tanemoto, K. and Maeda, T. (2003), "Aerodynamic characteristics of train/vehicles under cross winds", *J. Wind Eng. Ind. Aerod.*, **91**(1-2), 209-218.
Wu, M.X., Li, Y.L., Chen, X.Z. and Hu, P. (2014), "Wind spectrum and correlation characteristics relative to vehicles moving through cross wind field", *J. Wind Eng. Ind. Aerod.*, **133**, 92-100.
Xu, Y.L. and Ding, Q.S. (2006), "Interaction of railway vehicles with track in cross-winds", *J. Fluid.Struct.*, **22**(3), 295-314.
Yi, T.H., Li, H.N. and Gu, M. (2013), "Experimental assessment of high-rate GPS receivers for deformation monitoring of bridge", *Measurement*, **46**(1), 420-432.